PATHOLOGY ONCOLOGY RESEARCH
Vol 2, No 4, 1996

Science Press Publishing Ltd. TUDOMÁNY KIADÓ

ARTICLE

Mapping the Location of Prognostically Significant Microcirculatory Patterns in Ciliary Body and Choroidal Melanomas*

Robert FOLBERG,[1,2] Margaret FLECK,[3] Mary G MEHAFFEY,[1] Margaret MEYER,[1] Suzanne E BENTLER,[4] Robert F WOOLSON,[4] Jacob PE'ER[5]

Departments of Ophthalmology[1], Pathology[2], Computer Science[3], the Division of Biostatistics of the Department of Preventive Medicine[4], University of Iowa, Iowa City, IA, USA; and the Department of Ophthalmology[5], Hadassah-Hebrew University, Jerusalem, Israel

The microcirculation of choroidal and ciliary body melanomas is remodeled into architecturally distinctive patterns. The presence of two histologic microvascular patterns, networks and parallel vessels with cross-linking, is strongly associated with metastasis. This study was designed to test the hypothesis that networks and parallel vessels with cross-linking patterns are not distributed evenly throughout the tumor. From a set of 234 eyes removed for ciliary body or choroidal melanoma, 152 tumors contained at least one focus of either vascular networks or parallel vessels with cross-linking. Histological cross-sections were digitized and foci of tumor containing these patterns were pseudocolorized so that their location within the periphery or central tumor zone could be mapped. Ciliary body and choroidal melanomas vary widely in size and shape and it is not appropriate to describe the periphery of a tumor as a fixed value because in a small tumor, the periphery thus defined would occupy a larger percent area than in a larger tumor. In this study, the peripheral and central zones of each tumor were described by a function that was constant from tumor to tumor, allowing the width of the peripheral and central zones to vary proportionally with tumor size. Observed counts of vascular patterns per zone were compared statistically with expected counts based upon the percent area occupied by the peripheral and central zones. Discrete foci of networks and parallel with cross-linking vessels are over-represented in the tumor periphery ($p < 0.0001$). (Pathology Oncology Research Vol 2, No 4, 229–236, 1996)

Key words: melanoma, metastasis, prognosis, angiogenesis, vascularity, image analysis

Introduction

There are few descriptions of the localization of vascularization within tumors. In one experimental model of mouse mammary adenocinoma transplanted to skin, tumor vascularization developed at the tumor periphery.[1] In a histologic study of human radical prostatectomy specimens, prostatic carcinomas were found to be vascularized preferentially at the tumor center.[2]

Received: Oct 15, 1996, accepted: Nov 21, 1996

Correspondence: Robert FOLBERG, M.D.; University of Iowa, 100 Medical Research Center, Room 233, Iowa City, IA 52242-1182, USA, Tel (319) 335-7095; Fax: (319)335-7193; e-mail: robert-folberg@uiowa.edu

* Supported by National Institutes of Health Grant EY10457, Bethesda, Maryland, USA, and in part by an unrestricted grant from Research to Prevent Blindness, Inc., New York, New York, USA.

When an eye is removed for ciliary body or choroidal melanoma, the entire tumor and adjacent normal tissue are available for histologic study. It is therefore possible to map the location of prognostically important histologic features such as microcirculatory patterns. In ciliary body and choroidal melanomas, generation of the tumor microcirculation is a critical step in establishing metastases because there are no lymphatics within the uvea.[3] However, there is more to angiogenesis in choroidal and cilairy body melanomas than the production of new blood vessels: the microcirculation of these tumors remodels extensively,[4] producing microvascular patterns.

Nine microcirculatory patterns have been identified from histological sections of eyes removed for ciliary body and choroidal melanomas.[5,6] Two of these patterns, networks (defined as at least three back to back vascular loops) and parallel vessels with cross-linking, are very strongly asso-

ciated with death from metastatic melanoma.[6-8] It is not known if the microcirculatory patterns associated with metastasis in ciliary body and choroidal melanomas tend to develop in the tumor center, the periphery, or if they tend to be distributed equally throughout the mass.

There is a pressing practical need to determine if there is a preferential localization of microcirculatory patterns in ciliary body and choroidal melanomas. These tumors are among the few forms of cancer treated before a pathologist grades the neoplasm for biological aggressiveness. It is not possible to obtain incisional biopsies of the tumor without inflicting visual loss, and fine-needle aspiration biopsies do not yield material that is sufficiently representative to be of prognostic value.[9-11]

The development of non-invasive techniques to detect prognostically significant patterns might provide ophthalmologists with information to separate clinically those patients at high risk for metastasis from those at lower risk. Preliminary data suggest that two imaging techniques may be capable of detecting the presence of the prognostically significant microcirculatory patterns clinically. Power spectrum analysis of raw radiofrequency ultrasound data[12-14] may be used clinically to identify acoustic scatterers of certain sizes and concentrations in choroidal and ciliary body melanomas that correlate well with the presence of networks histologically.[15] Another technique, indocyanine green angiography augmented with digital scanning confocal fundus photography[16] may be capable of imaging directly the microcirculation of uveal melanomas situated posteriorly.[17]

This study was designed to determine if the prognostically significant microvascular patterns of networks and parallel vessels with cross-linking are distributed evenly throughout the choroidal and ciliary body melanomas, in the tumor periphery, or in the center of the tumor. This information may provide insight into the biology of angiogenesis and vascular remodeling in these tumors and may be useful in assisting those who are developing and implementing imaging techniques to detect these patterns clinically.

Material and Methods

Case selection and histological techniques

The cases used in this study were the same 234 cases used to investigate the relative prognostic significance of conventional histologic parameters of prognosis and vascular patterns; this dataset has been characterized previously.[6,18] Briefly, cases were excluded if the tumor involved only the iris, the lesion was a nevus, the tumor was more than 50% necrotic, representative material was not present in the paraffin blocks, the tumor had received pre-enucleation radiation therapy, the patient had more than one malignancy at the time of the enucleation, or the patient was enrolled in the Collaborative Ocular Melanoma Study.[19,20] The tenets of the Declaration of Helsinki were followed.

Two adjacent sections from each of these 234 tumors were stained with hematoxylin-eosin and the modified periodic acid-Schiff (PAS) without hematoxylin stain. The slide stained with the modified PAS reagent was used previously to detect vascular patterns as described previously,[5,6] and demonstration of microcirculatory patterns with this method, even after melanin bleaching in heavily pigmented tumors, has been shown to correlate with the identification of tumor microvessels stained with Ulex europaeus agglutinin I.[4,5,21,22] The slide stained with hematoxylin-eosin was used previously to measure the largest tumor dimension in contact with the sclera,[23] count mitotic figures, determine cell type,[24] and count the number of tumor infiltrating lymphocytes.[25]

From this dataset, 152 cases contained at least one focus of either networks or parallel with cross-linking patterns. Histological sections of these tumors were scanned digitally at 72 dots per inch resolution resulting in a magnification of X38 using a Nikon LS-3510 film scanner (Nikon, Inc, Electronic Imaging Department, Melville, NY, USA). Images were enhanced in the following manner using Adobe Photoshop, Version 3.0 (Adobe Systems, Mountainview, CA, USA) running under Microsoft Windows, version 3.11 (Microsoft Corporation, Bellvue, WA, USA) on a Hewlett-Packard Vectra 486 66-ST microcomputer (Hewlett-Packard, Palo Alto, CA, USA). The appearance of PAS positive microcirculatory patterns was enhanced by selecting the green channel, producing the same effect as introducing a green filter into the light path of a photomicroscope. The image was converted to a gray scale image and this positive image was converted to a negative image, rendering the vessels white against the dark background of the tumor stroma.[26]

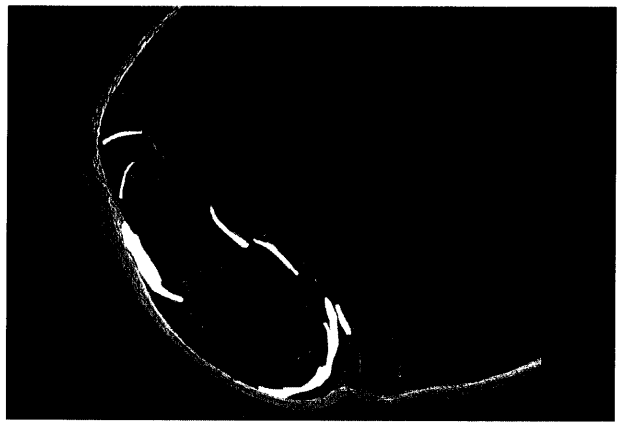

Figure 1. *Digitized image of a histologic cross section of a choroidal melanoma. This is a negative of the gray scale of this image. The two areas in the tumor occupied by networks have been colored red and the areas occupied by parallel with cross-linking have been colored yellow (PAS without hematoxylin, original magnification x38).*

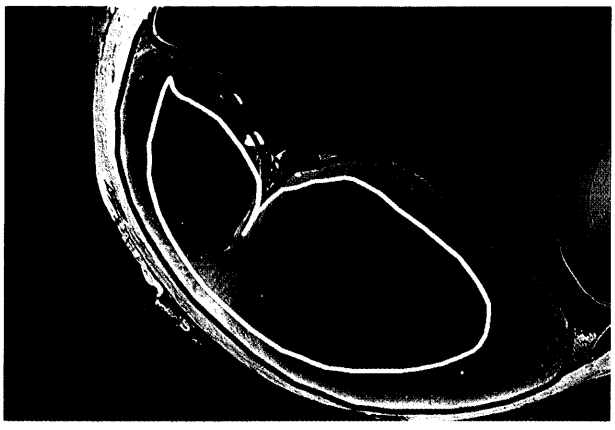

Figure 2. Digitized image of a histologic cross section of an irregularly shaped choroidal melanoma. The edge of the tumor has been traced in blue. The tracing of the edge was reduced by 25% and is represented in the yellow tracing that is fit within the tumor. Note that this technique does not generate a peripheral zone of uniform thickness around the circumference of the tumor (PAS without hematoxylin, original magnification x38).

Areas of the tumor containing networks and parallel with cross-linking patterns were painted on digital images of tumor cross-sections using the convention of coloring networks in red and parallel with cross-linking patterns in yellow *(Fig.1)*.

Mapping the Location of Prognostically Significant Patterns

An intuitive approach to describe the position of the vascular patterns within a tumor might involve reducing the image size of a tumor by a fixed percentage and fitting the reduced image inside the original tumor to fashion a peripheral zone. For example, one might attempt to trace the outline of a melanoma and reduce the area outlined by a fixed percentage. However, unless the melanoma is circular in outline, the reduction in size is not distributed uniformly along all vectors and the peripheral zone thereby defined is not distributed evenly within the tumor edge *(Fig.2)*.

It is also not appropriate to use absolute measurements to describe the peripheral zone of a melanoma. For example, if one defines the peripheral zone of a ciliary body or choroidal melanoma as a band with a width of 1 mm along the internal edge of a tumor, then the peripheral zone of a small tumor is proportionally wider than the peripheral zone of a larger tumor *(Fig.3)*.

In order to define the tumor periphery so that it is proportional to the size of the tumor but based on a function that is constant from tumor to tumor, the width of a peripheral zone was defined in this study as a fixed proportion of the diameter of the largest circle that could be fit within the outline of a tumor. For example, in the tumor illustrated in *Fig.4a*, the diameter of the largest circle that can be fit within the tumor is measured at 563 pixels. By theoretically rolling a circle along the inner edge of the tumor that is 1/8 the diameter of this largest circle fit (70 pixels), a peripheral zone was fashioned *(Fig.4b)*. In tumors that have tapered edges, the tumor tissue peripheral to outer zone is considered to be part of this outer zone *(Fig.4b and c)*.

Two additional concentric zones of bands, each 1/8 of the width of the largest circle fit within the tumor, were fashioned internal to the most peripheral zone; the remaining area was designated as the most central zone *(Fig.5)*. The technique used to create these zones with commercially available software is summarized in detail in *Table 1*.

For the purposes of recording location, each band was described by the color assigned to it (yellow, red, green

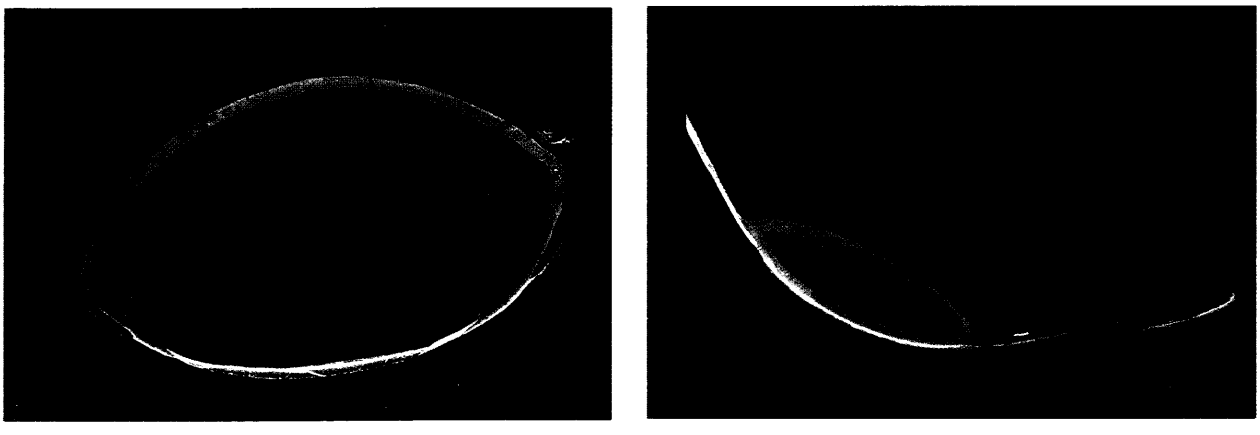

Figure 3. Digitized images of the histologic cross sections of two choroidal melanomas. A peripheral zone is painted with arbitrarily chosen fixed width of 0.38 mm. By defining the periphery as a band with a width fixed from tumor to tumor, the peripheral zone occupies less area in a large tumor (left) than a small tumor (right; both figures, PAS without hematoxylin, original magnification x38).

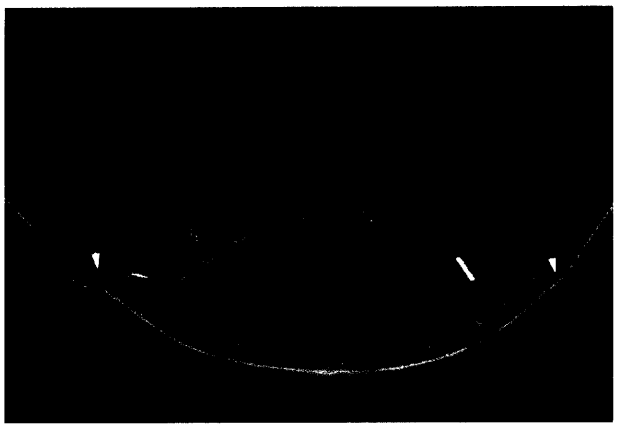

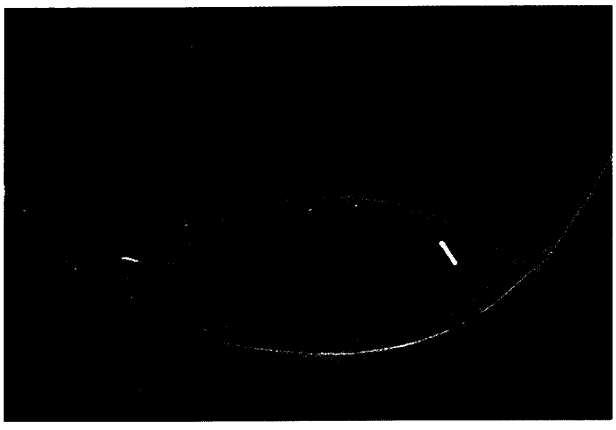

Figure 4. *Digitized images of the histologic cross section of one choroidal melanoma to illustrate the stages in creating zones. 4a. Areas in the tumor occupied by networks and parallel with cross-linking patterns are indicated in red and yellow respectively. The largest circle that can be fit within the contour of the tumor is indicated in blue. 4b. The most peripheral zone is painted in yellow at 26% opacity to permit the areas occupied by networks and parallel with cross-linking to be visualized. Note that by "rolling" a circle with a diameter equal to 1/8 the diameter of the largest circle that can be fit within the tumor, small zones are created in the tapering edges of the tumor that are not part of this peripheral zone (white arrowheads). These tips are considered by definition to be part of the peripheral zone. 4c. The tips are filled in with the color of the most peripheral zone. The inner three zones are fashioned according to the method outlined in Table 1 (all figures, PAS without hematoxylin, original magnification x38).*

and blue, representing most peripheral to central respectively, *Fig.5)*. A vascular pattern fully contained within one of the four mapping zones was designated as a discrete focus. A span was defined as a vascular pattern that crossed into more than one zone. Thus, a span of two zone crossings can be accounted for in a tumor in the following three ways: a pattern that extends from yellow to red, from red to green, or from green to blue. A span of three zone crossings can be accounted for in a tumor in only two ways: a vessel pattern that extends from yellow to red to green, or a pattern that extends from red, to green, to blue. A span of four zone crossings would be a vascular pattern that extends from yellow to red to green to blue.

The number of spans per tumor was recorded together with the locations of the zones affected by each span. *Fig.5* illustrates a tumor that contains foci of both parallel with cross-linking and networks. The tumor illustrated in *Fig.5* contains 2 foci of networks and one focus of parallel vessels with cross-linking in the most peripheral (yellow) zone, one focus of parallel vessels with cross-linking in the zone just interior to the most peripheral (red zone), two small spans of networks crossing two zones, from most peripheral to the zone just interior (crossing from yellow to red, upper left and bottom right of the tumor), and one large span of networks with three crossings from yellow to red, red to green, and green to blue.

Statistical Methods

In order to determine where the vessel patterns of networks and parallel with cross-linking develop in a tumor, descriptive analyses were performed, using chi-square tests for trend (observed number of foci or spans versus expected numbers of foci or spans). Comparisons were made for 2 and 3 zone crossings and for 2 zone crossings; no comparison was done for 4 zone crossings as there is only one way that such a span might occur in a tumor (yellow to red to green to blue).

The observed number of discrete vessel pattern foci per each zone were counted by summing the number of foci of the particular pattern in each zone in each tumor. The expected count per tumor was calculated by multiplying the total number of foci of either networks or parallel vessels with cross-linking found in the tumor by the proportion of cross-sectional area occupied by the zone of interest. For each tumor, the expected values were subtracted from the observed values and the result was summed over all tumors containing the vessel pattern of

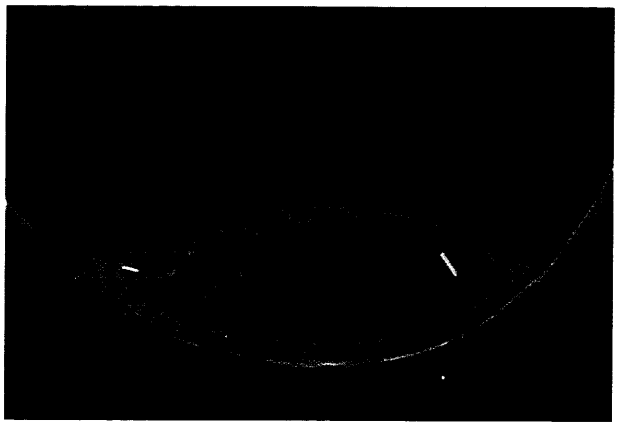

Figure 5. Same tumor as illustrated in Figure 4. All zones have been fashioned and are labeled according to the convention summarized in Table 1 (PAS without hematoxylin, original magnification x38).

interest (either networks or parallel vessels with cross-linking). The result (A) was squared and is the numerator of the chi-square statistic. The denominator (B) is the variance calculation per tumor summed over all tumors containing the particular vessel pattern.[27] The calculation of single degree of freedom chi-square statistic is therefore expressed by the formula

$$\chi^2 = A^2/B$$

$$\text{where } A = \sum_{1}^{k} (y_i - n_i\Pi_i) \text{ and } B = \sum_{1}^{k} n_i\Pi_i(1-\Pi_i).$$

In this formula, k equals the number of tumors with the particular vessel pattern *(i.e.*, for discrete foci of networks, k = 74 as there were 74 tumors that contained discrete foci of networks), y_i equals the number of vessel patterns of a particular type that are observed in a particular zone, n_i is the total number of vessel patterns of a particular type found anywhere in the tumor and P_i is the proportion of the cross-sectional area of the tumor accounted for by a given zone.

Spans of networks or parallel vessels with cross-linking, by definition, occupy more than one zone. In the calculation of chi-square statistics for spans, the observed number of spans equals the number of spans contained within the zones on either side of the zone crossing. For example, in a 2 zone crossing from yellow to red, the observed number of spans equals the number of spans detected in these two zones, and in a three zone crossing of yellow to red to green, the observed number of spans equals the number of spans detected in these three zones. The expected number of spans per tumor was calculated separately for spans of 2 and 3 zone crossings. For spans that crossed two zones, the expected number of spans in any given 2 zones equals the total number of spans that crossed two zones anywhere in the tumor multiplied by probability of the span falling in the two zones of interest. For example, for a span that crossed from the yellow to red zone, the probability of the span being in these zones is the sum of the proportional area of these two zone divided by the sum of the proportional areas of all contiguous two zone combinations within the tumor. The expected number of spans of 3 zone crossings is calculated similarly.

To adjust for multiple comparisons, p-values for the one degree of freedom chi-square test statistics for discrete foci and for spans of 2 zone crossings were calculated by referring this statistic to a chi-square with degrees of freedom determined by the size of the original contingency table (i.e., 3 degrees of freedom for foci and 2 degrees of freedom for spans of 2 zone crossings). This procedure controls the frequency of Type I errors in a conservative

Table 1.* Method to fashion zones for histological sections of ciliary body and choroidal melanoma

1. Digitize an image of the histological section of the tumor.[26]
2. Paint areas within the tumor containing networks and parallel with cross-linking patterns. It is helpful to use a separate color for each of these patterns (in this study, networks were indicated by red and parallel with cross-linking with yellow).
3. Add a layer to the image fashioned in step 2.
4. Software preferences are set to indicate the paintbrush size in pixels, and the largest circular paintbrush is fit within the tumor by trial and error. The diameter of the paintbrush in pixels is recorded. For very large tumors exceeding the maximum pixel size for the paintbrush, one may use the elliptical marquee tool which may be constrained to fashion the largest circle that can be fit inside the tumor. The diameter of a circle fashioned in this manner may be measured by the line tool set to zero pixels for line width. This number is the width of the peripheral band. In this study, the diameter of the largest circle was divided by 8 to create four zones. In practice, one may divide the diameter of the largest circle by 4 to create two zones (a periphery and a core), as the frequency distributions of patterns between two zones is statistically significant (see results).
5. Use the path tool to trace the circumference of the tumor using the "drag and click" method with the mouse. Make a selection from the path, then deselect the path.
6. Select a color (in this study, yellow is used for the outermost of the zones, but any color may be substituted) and fill at 26% opacity to avoid obscuring the underlying painted zones that identify the location of networks and parallel with cross-linking patterns. Contract the selection as often as necessary to contract the band by the number of pixels equal to the band width as calculated in step 4.
7. Select the clear function and fill with a different color (in this study, the zone internal to the yellow zone was colored red), and fill at 26% opacity as before.
8. Repeat steps 6 and 7 twice more until four zones are fashioned.
9. Select None, merge the layers, and save the image.

* This technique described below refers to functions in Adobe Photoshop, version 3.0 (Adobe Systems, Mountainview, CA) for illustrative purposes. Other software tools that accomplish the same effect may be substituted.

fashion and is used as the basis for the p-value calculations.[28] The critical values for the chi-square test statistics for spans of 3 zone crossings were determined using the value found for a chi-square with one degree of freedom.

Results

Of the 152 cases in this series that contained at least one span or focus of either networks or parallel with cross-linking, the two patterns associated with metastasis from choroidal and ciliary body melanomas,[6,7,18] 33 tumors (22%) contained only discrete foci and no spans, 28 tumors (18%) contained spans but no discrete foci, and 91 tumors (60%) contained both spans and discrete foci.

Table 2.* Comparison between number of expected and observed discrete foci and of vascular networks and parallel vessels with cross-linking

Zone	*Number of expected foci*	*Number of observed foci*	*Variance*	*Chi-square statistic*	*p*
Discrete foci: networks (74 tumors)					
Most peripheral (yellow)	98.19	159	54.7	67.60	<0.0001
Internal to peripheral (red)	65.79	37	46.3	17.89	0.0005
External to center (green)	43.87	24	35.2	11.22	0.0106
Center (blue)	15.15	3	14.0	10.54	0.0145
Discrete foci of parallel vessels with cross-linking (112 tumors)					
Most peripheral (yellow)	185.20	305	102.3	140.33	<0.0001
Internal to peripheral (red)	122.80	73	86.5	28.68	<0.0001
External to center (green)	81.27	31	65.3	38.72	<0.0001
Center (blue)	26.74	7	24.8	15.69	0.0013

* Zone colors correspond to scheme described in the text (see also Figure 5 for example). Number of Expected Foci is calculated as described in section on statistical methods. Degrees of freedom for chi-square for each individual comparison of observed and expected is 3 for p-value calculations. Overall chi-square statistic for networks is 107.25 with 3 degrees of freedom ($p < 0.0001$); overall chi-square statistic for parallel vessels with cross-linking is 233.425 with 3 degrees of freedom ($p < 0.0001$).

For discrete foci, both networks and parallel vessels with cross-linking are over-represented in the most peripheral zone, and under-represented in the three more interior zones (*Table 2*, overall chi-square p-value < 0.0001), indicating a clear tendency for these patterns associated with metastasis to form in the periphery. For spans that cross three zones (15 tumors had network spans of 3 crossings and 19 tumors had 3 zone crossings of parallel vessels with cross-linking), there is no significant trend for networks or parallel vessels to form either in the tumor periphery or in the center ($p = 0.2369$ and 0.0807 respectively). For spans that cross two zones, networks are distributed in both the periphery and in the tumor center as expected (*Table 3*, $p = 0.0715$ and $p = 0.4207$). For spans that cross two zones, parallel vessels with cross-linking are over-represented in the periphery (yellow and red) compared with the center (green and blue, *Table 3*, $p = 0.0001$ and 0.7293 respectively).

Discussion

The microcirculation architecture of choroidal and ciliary body melanomas may be used to describe tumor progression in this system. In the earliest primary melanocytic proliferations induced in the rabbit choroid by the repeated topical application of the chemical carcinogen, 7,12-dimethylbenz[a]anthracene (DMBA), melanocytes aggregated around normal pre-existing choroidal vessels. As the lesions grew, zones of avascularity developed within the lesions.[29,30] Similarly, human choroidal nevi contain only normal vessels, straight vessels, parallel arrangements of straight vessels without cross-linking, and avascular zones. Patients who have melanomas that contain only those microvascular patterns found in nevi have a significantly improved prognosis than those patients with melanomas that contain microcirculatory patterns not found in nevi (such as ares, ares with branching, closed vascular loops, networks and parallel vessels with cross-linking).[7] In Cox regression models, of the histologic

Table 3.* Comparison between number of expected and observed spans formed by vascular networks and parallel vessels with cross-linking

Zone crossing	*Sum of expected*	*Sum of observed*	*Variance*	*Chi-square*	*p*
Network spans crossing two zones (58 tumors)					
Most peripheral to next internal zone (yellow-red)	54.87	67	27.90	5.28	0.0715
Center to zone just external to center (blue to green)	20.36	15	16.6	1.73	0.4207
Parallel with cross-linking spans crossing two zones (96 tumors)					
Most peripheral to next internal zone (yellow-red)	110.23	142	55.56	18.16	<0.0001
Center to zone just external to center (blue to green)	39.52	35	32.4	0.631	0.7293

* Zone colors correspond to scheme described in the text (see also Figure 5 for example). Number of Expected Span Crossings is calculated as described in section on statistical methods. Degrees of freedom for chi-square for each comparison of observed and expected is 2 for p-value calculations.

variables studied including tumor size and cell type,[6,8,15] the detection of microvascular networks has the strongest association with metastasis. Therefore, not all forms of angiogenesis in this tumor system are associated with metastasis: remodeling of the microcirculation into networks and parallel vessels with cross-linking are, however, potent markers of tumor progression.

This study does not report the location of all expressions of tumor angiogenesis and is therefore not entirely parallel to studies that report tumor vascularization at the periphery[1] or in the tumor center.[2] This study does suggest that discrete foci of highly remodeled microvessels, networks and parallel with vessels with cross-linking, tend to appear in the periphery of the tumor, rather than in the central core. Spans may represent more advanced stages of vascularization and remodeling. Nevertheless, there is a tendency for shorter spans (two zone crossings) of parallel with cross-linking to appear in the two peripheral zones more frequently than expected by the proportion of area constituted by these zones.

The current study, localizing those microcirculatory patterns associated with metastasis (networks and parallel vessels with cross-linking) to the tumor periphery, may provide a foundation for a hypothesis concerning the biological events leading to their formation and an explanation for the association between pattern formation and metastasis. Studies of cultured human cutaneous melanoma cells suggest that a somewhat acidic environment favors invasion.[31] Additionally, cultured human uveal melanoma cells grown in an acidic environment are invasive into Type I collagen gels and are also capable of synthesizing Type VI collagen.[4] Type VI collagen is present in remodeling tissues and is considered to be responsible for pattern formation in the microcirculation and elsewhere in the stroma.[32]

Given the observation that the earliest ciliochoroidal proliferations incorporate pre-existing vessels, it is reasonable to postulate that with expansion of the lesion away from the central core, relative hypoxia in the tumor periphery upregulates factors responsible for angiogenesis, such as vascular endothelial growth factor (VEGF).[33,34] At the same time, local peripheral hypoxia and relative acidosis favor the deposition of extracellular matrix substances associated with remodeling of the microcirculation and stroma (such as Type VI collagen), and this microenvironment also favors the biological properties of tumor cell invasion.[4] The tendency for microvascular networks and parallel vessels with cross-linking to form in the tumor periphery and to be associated with metastasis is consistent with this proposed scheme.

It is difficult to describe precisely and quantitatively what is meant by the "periphery" of tumors that may vary in size and shape. In the study of prostatic carcinomas indicating that tumor vascularization was concentrated in the center rather than the periphery, the periphery was defined in terms of a fixed distance from the edge of the tumor.[2] In a large tumor, this distance would be proportionately less than for a small tumor *(Fig. 3)*.

In the current study, the periphery was described quantitatively by a function that could be applied consistently to each tumor, regardless of size or shape, instead of a fixed distance. The quantitative description of the tumor periphery was based a fixed percentage of the diameter of the largest circle fit inside the tumor's edges. Parenthetically, the periphery as defined by this function depends not only on the size of the tumor, but also the tumor's shape. For example, a relatively flat tumor with a large area of scleral contact would generate a peripheral zone that is thin. Likewise, a tumor that had a relatively narrow base but that was greatly elevated would contain a thin peripheral zone as defined by this technique.

In this study, an arbitrary fraction (1/8) of the diameter of the largest circle to fit within the tumor was selected as a starting point to generate four zones. This study indicated biological significance to this definition of the periphery as there was a clear tendency for discrete foci of networks and parallel vessels with cross-linking to appear in the most peripheral zone thus defined. However, in other tumor systems, it may be necessary to set the fraction of the largest circle fit within the tumor to another number to describe quantitatively zones of biological significance.

The technique used in this study to define the periphery of tumors quantitatively and describe the localization of prognostically significant microvascular remodeling patterns can be applied to other histopathological investigations that require localization of a feature of interest. Furthermore, this technique may be applied to ultrasonograms and in angiographic studies for pathology-imaging correlations. These correlations would be important in the development of non-invasive substitutes for biopsy for uveal melanomas.[12-17]

References

1. *Thompson WD, Shiach KJ, Fraser RA et al:* Tumours acquire their vasculature by vessel incorporation, not vessel ingrowth. J Pathol 151:323-332, 1987.
2. *Siegal JA and Brawer MK:* Topography of neovascularity in human prostate carcinoma. Cancer 75:2545-2551, 1995.
3. *Folberg R:* Tumor progression in ocular melanomas. J Invest Dermatol 100:326S-331S, 1993.
4. *Daniels KJ, Boldt HC, Martin JA et al:* Expression of Type VI collagen in uveal melanoma: role in pattern formation and tumor progression. Lab Invest 75:55-66, 1996.
5. *Folberg R, Pe'er J, Gruman LM et al:* The morphologic characteristics of tumor blood vessels as a marker of tumor progression in primary human uveal melanoma: a matched case-control study. Hum Pathol 23:1298-1305, 1992.
6. *Folberg R, Rummelt V, Parys-Van Ginderdeuren R et al:* The prognostic value of tumor blood vessel morphology in primary uveal melanoma. Ophthalmology 100:1389-1398, 1993.

7. *Rummelt V, Folberg R, Rummelt C et al:* Microcirculation architecture of melanocytic nevi and malignant melanomas of the ciliary body and choroid. A comparative histopathologic and ultrastructural study. Ophthalmology 101:718-727, 1994.
8. *Rummelt V, Folberg R, Woolson RF et al:* Relation between the microcirculation architecture and the aggressive behavior of ciliary body melanomas. Ophthalmology. 102:844-851, 1995.
9. *Augsburger JJ, Shields JA, Folberg R et al:* Fine needle aspiration biopsy in the diagnosis of intraocular cancer cytologic-histologic correlations. Ophthalmology 92:39-49, 1985.
10. *Folberg R, Augsburger JJ, Gamel JW et al:* Fine-needle aspirates of uveal melanomas and prognosis. Am J Ophthalmol 100:654-657, 1985.
11. *Char DH, Kroll SM, Stoloff A et al:* Cytomorphometry of uveal melanoma. Comparison of fine needle aspiration biopsy samples with histologic sections. Anal Quant Cytol Histol 13:293-299, 1991.
12. *Coleman DJ and Lizzi FL:* Computerized ultrasonic tissue characterization of ocular tumors. Am J Ophthalmol 96:165-175, 1983.
13. *Coleman DJ, Rondeau MJ and Silverman RH:* Computerized ultrasonic bimometry and imaging of intraocular tumors for the monitoring of therapy. Tr Am Ophthalmol Soc 85:49-81, 1987.
14. *Coleman DJ, Silverman RH, Rondeau MJ et al:* Ultrasonic tissue characterization of uveal melanoma and prediction of patient survival after enucleation and brachytherapy. Am J Ophthalmol 112:682-688, 1991.
15. *Coleman DJ, Rondeau MJ, Silverman RH et al:* Correlation of microcirculation architecture with ultrasound parameters of uveal melanoma. Eur J Ophthalmol 5:96-106, 1995.
16. *Bartsch D, Weinreb RN, Zinser G and Freeman WR:* Confocal scanning infrared laser ophthalmoloscopy for indocyanine green angiography. Am J Ophthalmol 120:642-651, 1995.
17. *Schneider U, Gelisken F, Inhoffen W et al:* Indocyanine-green videoangiography of malignant melanomas of the choroid using the scanning laser ophthalmoscope. Ger J Ophthalmol 5:6-11, 1996.
18. *Pe'er J, Rummelt V, Mawn L et al:* Mean of the ten largest nucleoli, microcirculation architecture, and prognosis of ciliochoroidal melanomas. Ophthalmology 101:1227- 1235, 1994.
19. *Fine SL:* How should we manage a patient with uveal melanoma (editorial). Arch Ophthalmol 103:910-911, 1985.
20. *Fine SL:* No one knows the preferred management for choroidal melanoma. Am J Ophthalmol 122:106-108, 1996.
21. *Rummelt V, Gardner LM, Folberg R et al:* Three-dimensional relationships between tumor cells and microcirculation using double cyanine-immunolabeling, laser scanning confocal microscopy and computer-assisted reconstruction: an alternative to cast corrosion preparations. J Histochem Cytochem 42:681-686, 1994.
22. *Folberg R, Mchaffey M, Gardner LM et al:* 1996.The microcirculation of choroidal and ciliary body melanomas. Eye (in press)
23. *Folberg R, Gamel JW, Greenberg RA et al:* Comparison of direct and microslide pathology measurements of uveal melanomas. Invest Ophthalmol Vis Sci 26:1788-1791, 1985.
24. *McLean IW, Foster WD, Zimmerman LE et al:* Modifications of Callender's classification of uveal melanoma at the Armed Forces Institute of Pathology. Am J Ophthalmol 96:502-509, 1983.
25. *de la Cruz PO, Jr, Specht CS and McLean IW:* Lymphocytic infiltration in uveal malignant melanoma. Cancer 65:112-115, 1990.
26. *Montague PR, Meyer M and Folberg R:* Technique for the digital imaging of histopathologic preparations of eyes for research and publication. Ophthalmology 102:1248-1251, 1995.
27. *Rosner B:* Fundamentals of Biostatistics. Wadsworth, Belmont, CA, 345, 1995.
28. *Grizzle JE, Starmer CF and Koch GG:* Analysis of categorical data by linear models. Biometrics 25:489-505, 1969.
29. *Folberg R, Baron J, Reeves RD et al:* Primary melanocytic lesions of the rabbit choroid following topical application of 7, 12-dimethylbenz[a]anthracene: preliminary observations. J Toxicol Cutataneous Ocul Toxicol 9:313-334, 1990.
30. *Pe'er J, Folberg R, Massicotte SJ, Baron J et al:* Clinicopathologic spectrum of primary uveal melanocytic lesions in an animal model. Ophthalmology 99:977-986, 1992.
31. *Martinez-Zaguilan R, Seftor EA, Seftor REB et al:* 1996.Acidic pH enhances the invasive behavior of human melanoma cells. Clin Exp Met 14:176-186, 1996.
32. *Zhang LQ, Laato M, Muona P et al:* Normal and hypertrophic scars: quantification and localization of messenger RNAs for type I, III and VI collagens. Br J Dermatol 130:453-459, 1994.
33. *Dvorak HF, Sioussat TM, Brown LF et al:* Distribution of vascular permeability factor (vascular endothelial growth factor) in tumors: concentration in tumor blood vessels. J Exp Med 174:1275-1278, 1991.
34. *Dvorak HF, Detmar M, Claffey KP et al:* Vascular permeability factor/vascular endothelial growth factor: An important mediator of angiogenesis in malignancy and inflammation. Int Arch Allergy Immunol 107:233-235, 1995.